JOURNAL OF MATERIALS SCIENCE 16 (1981) 1151–1166

The structure and mechanical properties of an injection-moulded acetal copolymer

J. BOWMAN
Department of Non-Metallic Materials, Brunel University, Kingston Lane, Uxbridge, UK

Processing conditions, microstructure and mechanical property correlations have been explored in injection-moulded plaques of an acetal copolymer. Barrel temperature was varied systematically between 453 and 503 K, with a constant mould temperature of 343 K. The microstructure and texture were determined by polarized light microscopy and X-ray pole-figure analysis, respectively. The overall structure of the mouldings was layered through the thickness and symetrical about the moulding centre line. At all barrel temperatures five layers were present: the outer three layers possessed significant preferred chain-axis orientation in the crystalline phase, while the two layers at the centre of the moulding were equiaxed. The texture and morphology of each layer is described and related to a model of mould filling. Increases in the barrel temperature reduced the extent of the outer oriented layers while increasing the extent of the equiaxed layers. Tensile tests were conducted on samples taken at 0° and 90° to the injection direction. Increases in barrel temperature had no influence on modulus but decreased both ($\alpha = 0$ and 90°) engineering yield stresses. The yield stress could be correlated with the extent of the oriented layers within mouldings. At all barrel temperatures the yield stress was greater when $\alpha = 90°$; this behaviour is explained in terms of a composite model.

1. Introduction

Processing semicrystalline plastics may suppress crystallization and/or introduce preferred texture into part or all of the moulded component. In injection moulding both cases have been observed: nylon 6 and poly(butyleneteraphthalate) mouldings exhibit a low-crystallinity or amorphous surface layer, with little [1–3] or no [4] evidence of preferred chain-axis orientation, and a crystalline equiaxed core, the extent of which varies with moulding conditions; mouldings of polyethylene [5–7], polypropylene [8–10], polyoxymethylene [11, 12] and TPX, a copolymer of poly-4-methylpentene-1, [13, 14] produce complex multi-layered structures. All layers are crystalline and those nearest the moulding surface are the most highly oriented. Layer extent, and the parallelism of the chain-axis with the machine direction, are both a function of moulding conditions. This suppression of crystallization and/or the introduction of a preferred texture can alter the physical properties and states of the moulded components. In nylon 6 injection mouldings, a reversal of sign of the residual stress distribution occurred after exposing the mouldings to water [4], differential crystallization in the nylon 6 induced this potentially catostrophic reversal of surface stress. For tensile testing parallel to the machine direction, a ductile to brittle transition in the mechanical properties of injection mouldings of TPX was effected when the barrel temperature was increased by only 20° C [14, 15] during moulding, the transition being associated with a band of structure near the centre of the moulding where the chain axis was oriented perpendicular to the direction of injection. Changes in the modulus [16–18], tensile strength [9, 18] and impact resistance [4, 18] have also been recorded as moulding conditions and moulding microstructure varied in injection mouldings of semicrystalline plastics.

For polyoxymethylene, or acetal, a semicrystalline thermoplastic, relationships between moulding conditions, moulding microstructure and component mechanical properties in injection mould-

0022–2461/81/051151–16$03.60/0

ings have also been established. The influence of mould temperature on the microstructure and mechanical properties of Delrin, an acetal homopolymer, has been investigated and reported by Clark [11, 12, 19], while Bohme [20], again for Delrin, notes the influence of mould temperature and injection pressure. In these papers, injection-moulded acetals exhibited a complex multilayered microstructure, with all of the strata exhibiting crystallinity; that is, acetal mouldings belong to the second group defined in the first paragraph. In these type of mouldings it appears that barrel temperature exerts the most powerful influence, of all practical moulding variables, on microstructure and mechanical properties for a single grade of plastic [16 18]. The influence of barrel temperature on the microstructure and the mechanical properties of injection mouldings of an acetal copolymer has therefore been examined in some detail and the results are reported in this paper. From observations of the changes in microstructure with barrel temperature, the formation of the microstructure is explained in terms of mould filling and melt cooling.

2. Material, mould and injection moulder

Acetal is marketed as both a homopolymer and copolymer; random sequences of CH_2–CH_2 bonds, incorporated into the main chain, define the copolymer. The copolymer has increased thermal stability and processability and was therefore used in this study; the copolymer was supplied by the Polymer Characterization Unit of the Rubber and Plastics Research Association (RAPRA), UK. Acetal homopolymer can exist in two crystalline, hexagonal and orthorhombic, forms. Both phases are stable at room temperature, but above 333 K the orthorhombic is thought to revert to the hexagonal [21]. Low-temperature deformation of the hexagonal acetal can induce the presence of the orthorhombic phase [22]. The dimensions of the unit cell of the hexagonal phase of acetal homopolymer are taken as those of Andrews and Martin [23], with $a = 4.478$ Å and $c = 17.3$ Å. These dimensions vary little for the copolymer [24]. The lattice parameters of the orthorhombic acetal homopolymer are in dispute: Carazzolo and Mammi [25] quote $a = 4.77$ Å, $b = 7.65$ Å and $c = 17.8$ Å, while Harris and Bevis [26] assume the c axis retains its hexagonal length of 17.3 Å, so that $a = 4.96$ Å and $b = 7.44$ Å. The density range for the fully amorphous to the theoretical crystalline hexagonal phase of the homopolymer is 1250 to 1486 kg cm^{-3} [24] with a melting temperature for the copolymer of 436 K.

The acetal copolymer was injection moulded into a 2.5 mm thick, double-sided, flash-gated, 76 mm square, plaque mould (Fig. 1). A PECO 21 MR injection moulder, owned by and sited at RAPRA, UK, was used for moulding. Screw type "A" was used to give a shot weight (polystyrene equivalent) of 78 g, a maximum injection pressure of 112 MN m^{-2} and a rate of injection of 1.07×10^5 mm^3 sec^{-1}. The locking force was 80 tonne.

3. Experimental procedure

3.1. Moulding

The acetal copolymer was moulded at six barrel temperatures: 453, 463 473, 483, 493 and 503 K, all with one mould temperature of 343 K. The line pressure varied between 4.3 and 4.9 MN m^{-2} and the screw back pressure between 1.52 and 3.17 MN m^{-1}. Packing pressure was maintained for 10 sec for the 453 K moulding, 25 sec for 463, 473 and 483 K mouldings and 30 sec for the 493 and 503 K mouldings (mouldings are identified by the barrel temperature). The cooling time was constant at 20 sec.

3.2. Optical microscopy

The microstructures of the injection-moulded acetal copolymer specimens were examined by polarized light microscopy of thin microtomed slices. Thin slices were prepared by microtomy using a Leitz sledge microtome with slices microtomed to thicknesses of 2–6 μm off the z–y and z–x planes (see Fig. 2). Cut slices were uncurled mechanically, immersed in lens oil ($\mu = 1.472$) and sandwiched between a glass slide and cover slip. A Leitz Zetopan

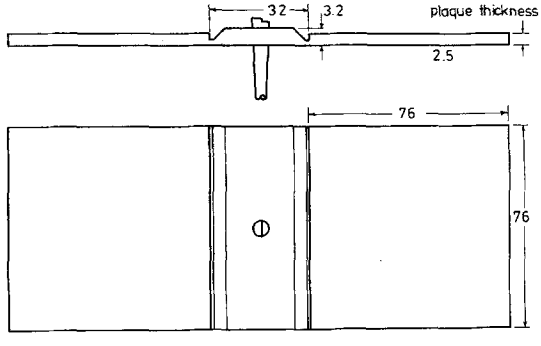

Figure 1 Shape and dimensions (in millimetres) of the plaque mould.

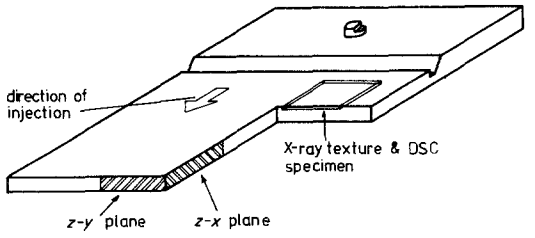

Figure 2 Schematic presentation of the moulding showing the z–y and z–x planes from which the microtomed samples were taken, together with the position and orientation of the X-ray pole figure specimen.

microscope was set up for transmission polarized light microscopy with the polarizer and analyser crossed.

3.3. Differential scanning calorimetry (DSC)

Polarized light microscopy of thin microtomed slices revealed a layered structure through the thickness of the moulding. Selected layers were isolated by polishing [14]. The melting temperature of these layers was determined using a Perkin-Elmer DSC-1B, calibrated with indium, whose melting point (429 K) is close to the melting temperatures of acetal copolymers. The heating rate was 4° C min^{-1}, and the sensitivity employed was 8 mcal sec^{-1} for a sample of weight 4 to 5 mg.

3.4 X-ray poly-figure analysis

X-ray analysis based on the determination of pole figures using an X-ray diffractometer is becoming widely used for the texture investigations of rolled [21, 27, 28] and injection-moulded semicrystalline plastics [6, 14, 15, 29]. Pole figures from selected layers were produced by mapping the distribution of the (1 0 $\bar{1}$ 0) planes; the (1 0 $\bar{1}$ 0) inter-plane spacing was 3.87 Å and the Bragg angle was 23°. The pole figures were produced with a Schulz texture goniometer (Phillips Model PW1078) employing nickel-filtered CuKα radiation [30, 31]. Data collection for pole-figure mapping was as described by Preedy and his co-workers [32].

3.5. Density measurements

Material of an idiosyncratic shape was cut from each of the six barrel-temperature mouldings. The density was determined in a carbon tetrachloride/ethanol column whose range at 296 K was 1240 to 1500 kg m^{-3}. Two specimens were used for each moulding condition and measurement was made two hours after immersion.

3.6. Tensile testing

Tensile specimens, to ASTM D638 Type IV standard, were cut from the plaques at 0° and 90° to the direction of injection. Tensile specimens were mounted in serated grips and tested at a cross-head speed of 5 mm min^{-1} (2.5×10^{-3} sec^{-1} initial strain rate) on an INSTRON (floor model TTCM). The temperature of testing was 294 K. At each barrel temperature at least six specimens were tested and from the load–time curves the Young's modulus and the engineering yield stress were calculated.

4. Results

4.1. Structures present

Table I tabulates the five structures identified within the moulded acetal copolymer plaques. In Fig. 3 polarized light photomicrographs from a 483 K barrel-temperature moulding highlight the morphologies of Structures 1 to 5, and the corresponding (1 0 $\bar{1}$ 0) pole figures are presented in Fig. 4. Note that the thickness of the layer of Structure 1 limited the possibility of obtaining a pole figure, or DSC curve, safely from that layer.

A quantitative measure of the preferred crystal orientation within the different layers is given in Table I by $\langle\cos^2\theta_{md}\rangle$, where θ is the angle averaged between the (1 0 $\bar{1}$ 0) planes normals and the machine/injection direction [6, 29, 33]. In this study the computer programme used to map the pole figures also determined $\langle\cos^2\theta_{md}\rangle$.

The Bravais lattice of acetal and its copolymers is normally hexagonal with only one independent orientation function [33, 34], so that the preferred chain-axis orientation of the various layers within the mouldings can be assessed from a knowledge of $\langle\cos^2\theta_{md}\rangle$. When $\langle\cos^2\theta_{md}\rangle$ is equal to $\frac{1}{3}$, the crystal orientation is random, and for the (1 0 $\bar{1}$ 0) reflections when $\langle\cos^2\theta_{md}\rangle$ is zero, the chain axis is aligned parallel to the injection/machine direction. If the value of $\langle\cos^2\theta_{md}\rangle$ were unity, then the preferred chain orientation would be perpendicular to the machine direction. Table I indicates that Layers 4 and 5 had little preferred chain-axis orientation, while Layer 3 was oriented, but not as highly oriented as Layers 1 and 2; the preferred direction of orientation of the chain axis in Layers 1 and 2 and Layer 3 was almost parallel with the injection direction.

The DSC melting curves from Layers 1 and 2 to Layer 5 showed the melting temperature increasing through the thickness of the moulding. There was no evidence of a high-temperature melting

TABLE I Microstructure and properties of layers present in injection-moulded acetal copolymer plaques

Layer	1	2	3	4	5
Morphology*	Featureless and bi-refringent	Oriented spherulites growing away from mould wall	Fine	Spherulitic; size a function of melt temperature	Fine, but spherulites observable
Spherulite size (diameter along direction of injection)	–	Increasing from 10 to 30 μm as melt temperature increases	–	Maximum increasing from 14 to 40 μm with melt temperature	Maximum increasing from 20 to 70 μm with melt temperature
$\langle\cos^2\theta\rangle_{md}$ for $(1\,0\,\bar{1}\,0)$ reflections	0.164†	0.164†	0.230‡	0.327‡	0.316‡
$(1\,0\,\bar{1}\,0)$ pole figures; positions of poles	3 main poles on the equator 60° apart. One pole on specimen normal		2 poles on equator 135° apart, equal about specimen normal	No clear texture	No clear texture
Peak in DSC melting curve	Single peak at 434.4 K, 436.5 K on re-melting		Single peak 435/436 K, reheated 437 K	Single peak at 436 K	Single peak at 437 K
Density§ (plaque density 1406 kg m^{-3})	1397 to 1405 kg m^{-3} as barrel temperature varies		–	–	–

* As revealed by polarized light microscopy of microtomed sections.
† Average from all barrel temperatures.
‡ Average from four lowest barrel temperatures.
§ Plaque density was insensitive to barrel temperature.

peak in the outer layers. Reheated, the samples from Layers 1 and 2 and Layer 3 gave higher melting temperatures. The density of the outer layers was close to the overall plaque density of 1406 kg m^{-3}.

4.2. The influence of barrel temperature on the extent of structures 1 to 5

The Structures 1 to 5 have been identified in Section 4.1 and Table I. Fig. 5 plots the extent and occupancy (in per cent) of Structures 1, 2 and 3 and Structures 4 and 5 as two groups. Figs 6a and 6b plot the extent of structures 1 to 5. From Table I and Figs 5 and 6 it is observed that:

(a) Structures 1, 2 and 3 were the most highly oriented, and all decreased in extent with increasing barrel temperature.

(b) Structures 4 and 5 possessed little preferred crystal orientation, and both increased in extent with increasing barrel temperature.

4.3. Changes in texture and microstructure induced by barrel temperature

4.3.1. Layers 1 and 2

Increasing the barrel temperature increased the size of the preferred-growth spherulites in Layer 2: the microstructure of Layer 1 was not seen to change. The texture of Layers 1 and 2 changed with barrel temperature. At low barrel temperatures the $(1\,0\,\bar{1}\,0)$ pole figures indicated that the chain axis in the crystalline phase was aligned parallel to the injection direction, while one of the $(1\,0\,\bar{1}\,0)$ plane normals alinged parallel to the mould surface normal. This biaxial orientation faded at higher barrel temperatures, but the chain axis retained its preferred orientation (Fig. 7).

4.3.2. Layer 3

Layer 3 had a morphology that was termed fine (see Table I) and optical microscopy failed to reveal any major changes in microstructure with

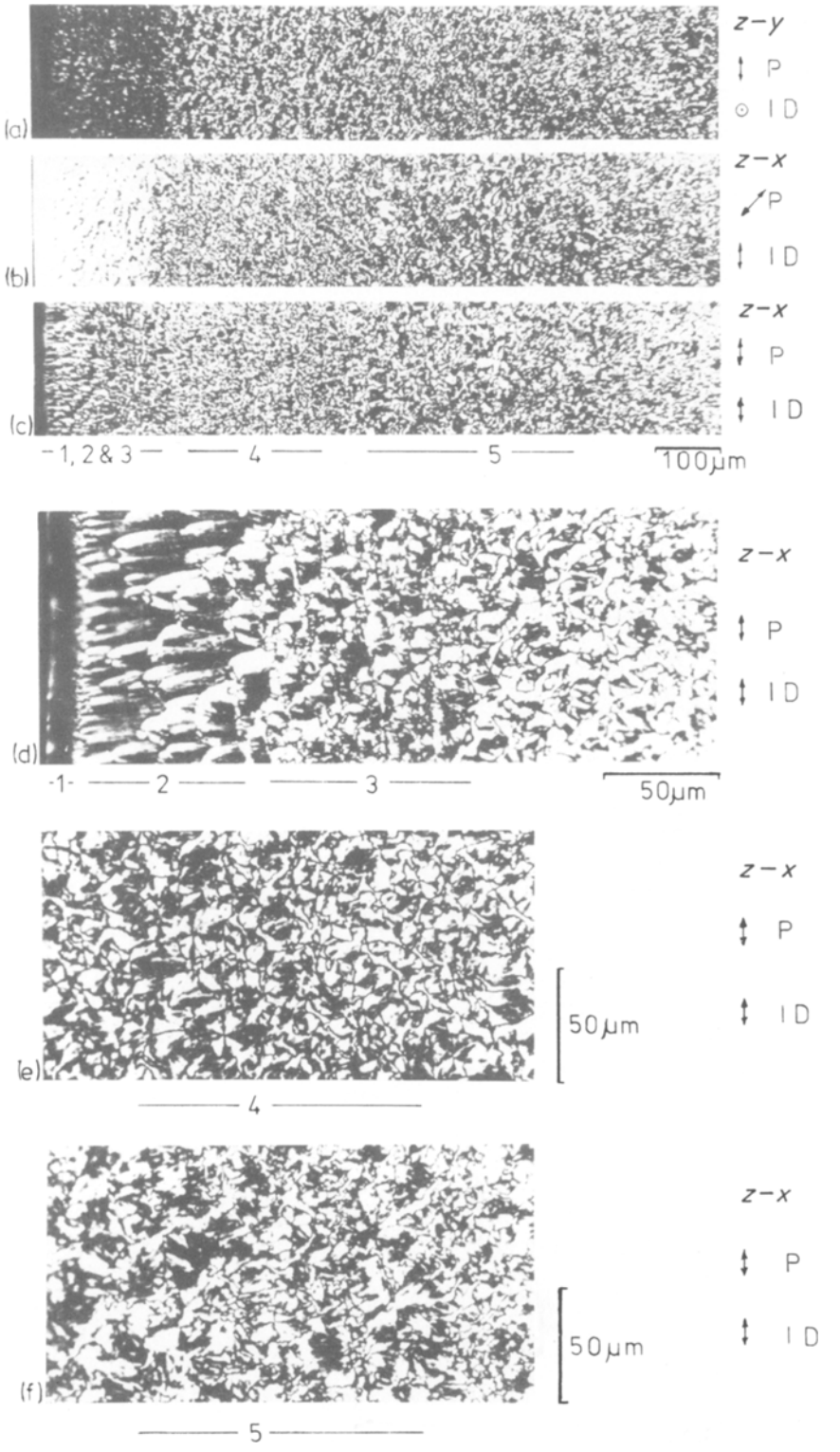

Figure 3 Low magnification optical photomicrographs [(a), (b) and (c)] of the 483 K barrel temperature moulding showing the macrostructure and the broad division between the bi-refringent outer oriented layers 1, 2 and 3, and the non-oriented centre layers. Optical photomicrographs of Layers 1 to 5 are shown in (d), (e) and (f). The injection direction (ID), the direction of vibration of the polarized light (p) and the plane from which the microtomed sample was taken are identified.

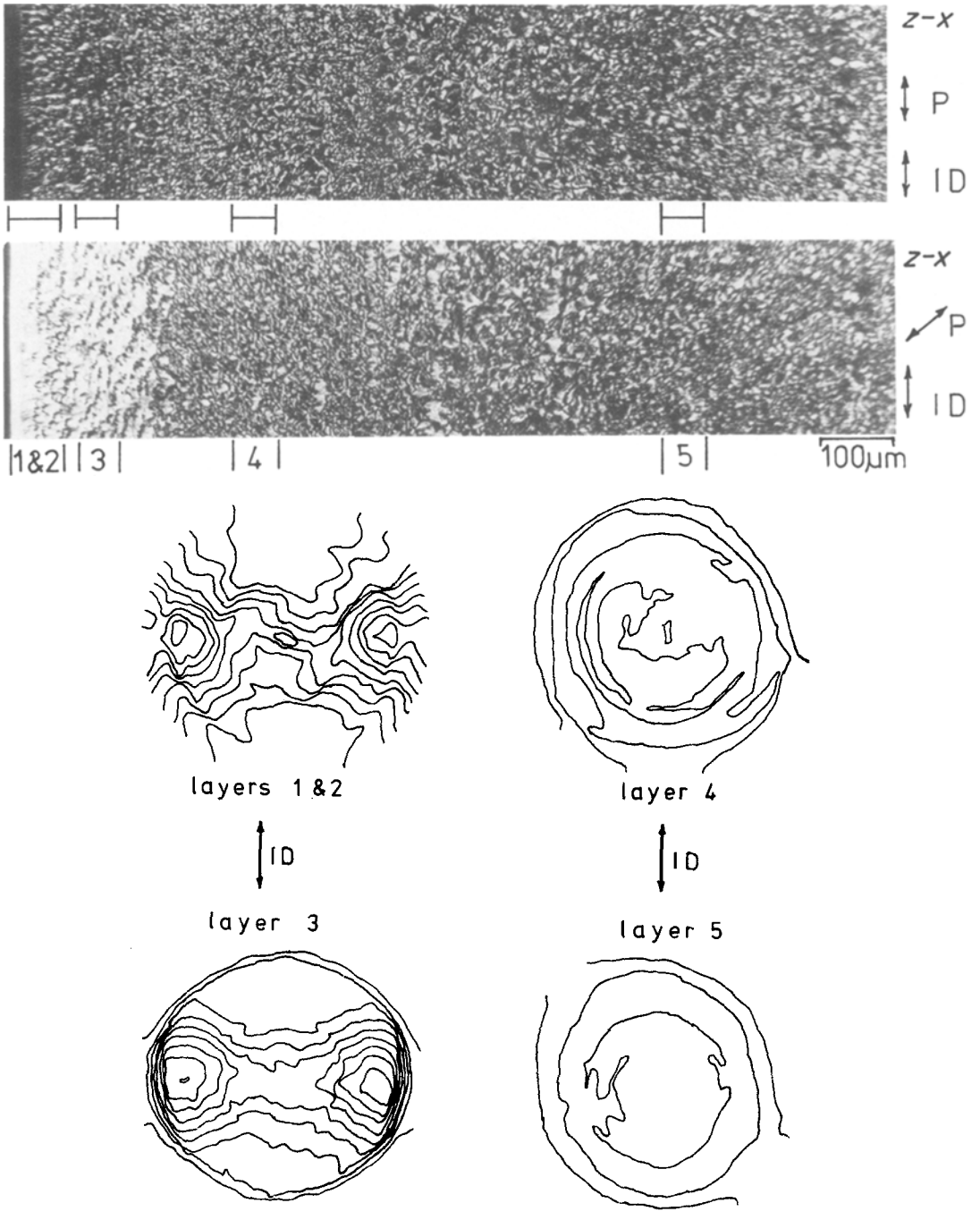

Figure 4 Optical micrographs from the 483 K barrel temperature mouldings together with the $(10\bar{1}0)$ pole figures of Layers (1 and 2), 3, 4 and 5.

barrel temperature. Similarly, the $(10\bar{1}0)$ pole figures of Layer 3 failed to show any major changes as the barrel temperature was increased from 453 to 483 K. The two poles were still present, as in Fig. 4, the angle between them being insensitive to barrel temperature.

4.3.3. Layers 4 and 5

Layer 4 coarsened with increasing barrel temperature (Fig. 8), the maximum observed spherulite size increasing as shown in Table I. In Layer 5 increases in barrel temperature increased spherulite size, as noted in Table I, there being a tendency

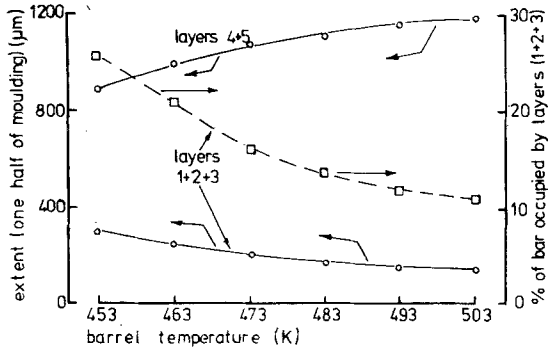

Figure 5 The influence of moulding conditions on the extent of the oriented (1, 2 and 3) and the equiaxed (4 and 5) layers.

for the structure to be more clearly spherulitic with increasing barrel temperature (Fig. 9).

4.4. Mechanical properties of mouldings

At all barrel temperatures the modulus perpendicular to the injection direction was greater, by between 5 and 10%, than the modulus parallel to the injection direction, the barrel temperature exerting little influence. Both barrel temperature and α, the angle between the tensile axis and the injection direction, exerted an influence on tensile strength (Fig. 10), deformation mode and fracture surface morphology (Fig. 11). For samples pulled at 90° to the injection direction ($\alpha = 90°$) all samples exhibited surface crazing, had a flat fracture surface and failure appeared to initiate at the surface (Fig. 11a and b). For $\alpha = 0°$, no surface crazing could be observed. The fracture surface showed evidence of drawing with barrel temperature exerting some influence (Fig. 11c and d), and failure initiating in the centre of the moulding.

5. Discussion

5.1. Overall moulding structure

The mechanism by which a plastic melt fills a cold mould, of constant cross-section, is generally accepted to be one whereby a slow-moving or stationary surface layer is deposited continuously as the melt front progresses down the mould, the core of the moulding, especially near the gate, being the last to fill [35, 36]. Computer studies of mould filling have highlighted the presence of this slow-moving or stationary skin by presenting temperature, velocity and shear-rate profiles through the thickness of a moulding [37–40]. Experimental work has, as far as is possible, shown that the concept of a stationary outer skin, present during the filling of the mould, is correct (as long as jetting does not occur) [40–43]. The extent, through the thickness of a moulding, of the stationary skin has been shown to vary with injection rate [39], mould temperature [37, 38], injection pressure [38] and melt temperature [38]. Increases in melt temperature were computed to reduce the extent of the stationary skin.

A model for the deposition of the stationary skin has been proposed by Tadmor [36]. The filling process is divided into local flow at the melt front, which gives the skin of the moulding, and flow behind the melt front between the already frozen skins, to give the core. Consider first skin formation: the melt core behind the front travels faster than the front and on reaching and becoming the front undergoes a fountain-type of flow which is extensional in character [44]. The macromolecules of the melt that form the skin, in undergoing extensional flow at the melt front, are aligned nearly parallel to one another, and the preferred chain-axis orientation is preserved as the

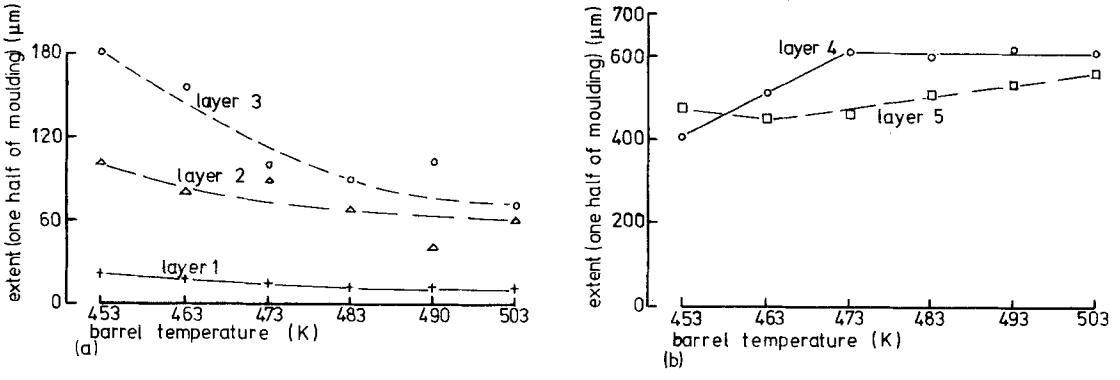

Figure 6 The influence of barrel temperature on the extent of the individual layers. (a) Layers 1, 2 and 3; (b) Layers 4 and 5.

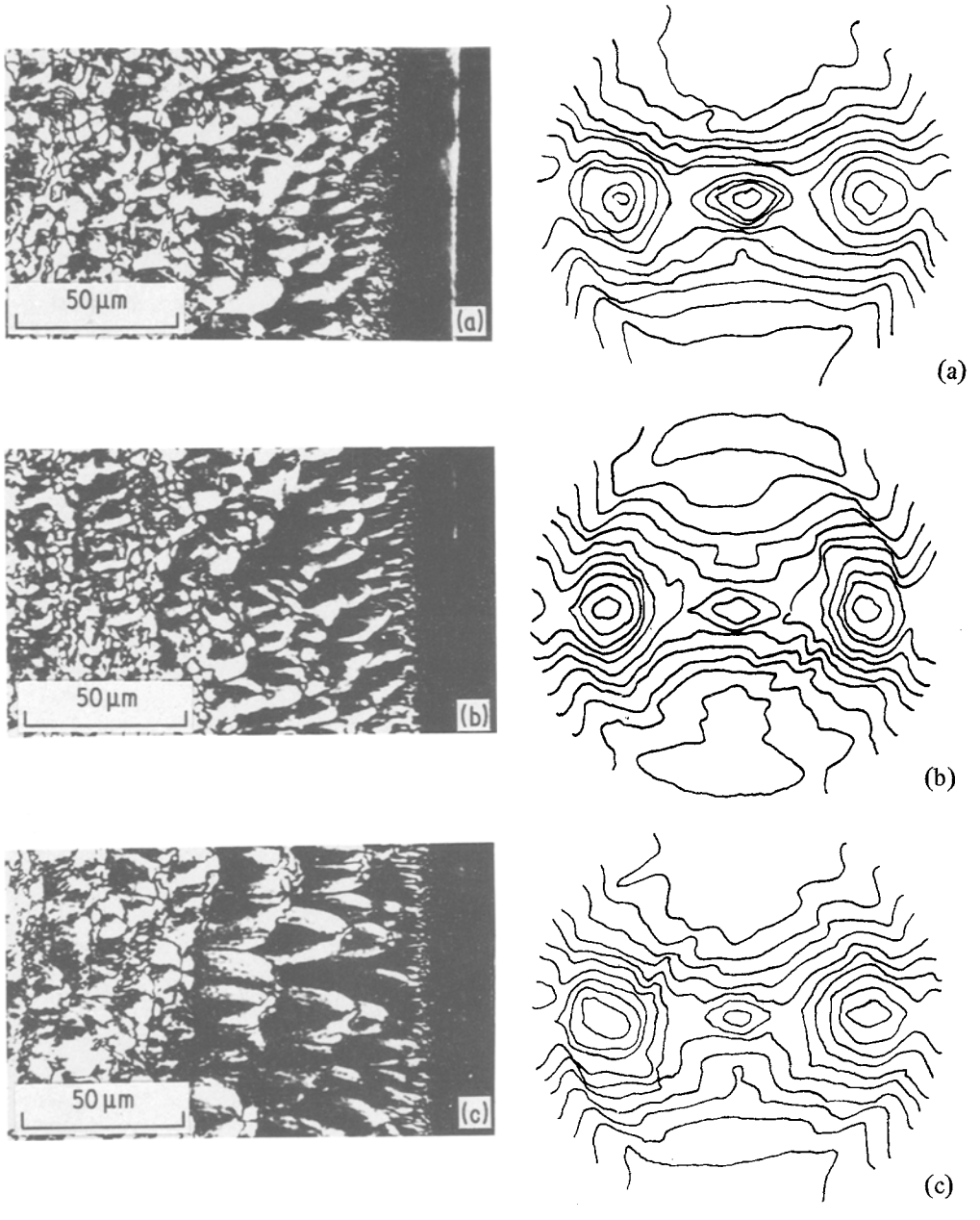

Figure 7 Optical micrographs and the accompanying $(10\bar{1}0)$ pole figures of Layers 1 and 2 showing, for three barrel temperatures the influence of processing conditions on morphology and texture. (a) 453 K, (b) 473 K, (c) 493 K.

melt freezes on touching the cold mould wall. Melt deposited further from the mould wall is still oriented but cools more slowly, so relaxation occurs and some of its preferred chain-axis orientation is lost. Note, however, that for some mouldings the maximum preferred orientation is just below the moulded surface [7].

Consideration is now given to the structure in the core of the moulding. The melt that forms the core of a moulding has passed between the stationary and cooling skins. This flowing melt has a velocity and shear-rate profile that has zero shear adjacent to the skins and at the centre of the moulding, with maximum shear in between (Fig. 12). The structure of some injection mouldings of amorphous polystyrenes was used as the basis for Tadmor's hypothesis [45, 46].

In these acetal copolymer mouldings the three outer layers, Layers 1, 2 and 3 (see Table I and Figs 3 and 4), were the most highly oriented and all

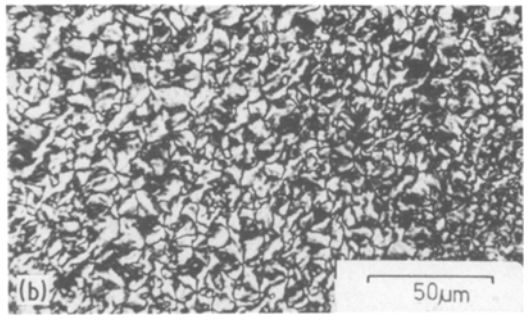

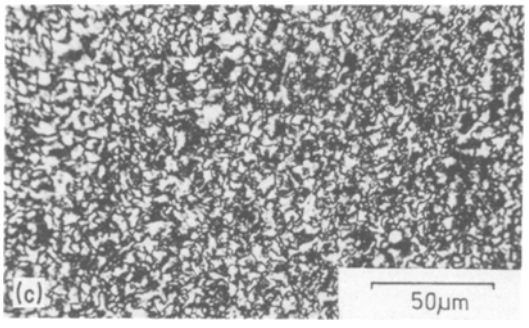

Figure 8 The influence of barrel temperature on the morphology of Layer 4. (a) 493 K, (b) 473 K, (c) 453 K.

decreased in extent with increasing barrel temperature (Figs 5 and 6). The two inner most layers, Layers 4 and 5, possessed the least preferred chain-axis orientation (Table I) and both these layers increased in extent with increasing barrel temperature. In the light of Tadmor's model and the computer simulations of mould-filling, it is proposed that the outer two layers (and possibly the third) formed the "skin" of the moulding. That is, during the filling process these layers constituted the stationary or slow-moving polymer, while the moulding core was composed of Layers 4 and 5 (see Fig. 12a and b).

5.2. Microstructures of the individual layers

5.2.1. Layer 1

The fine structure of the bi-refringent Layer 1 was not examined, but it was assumed that the layer was crystalline and further assumed that the $(10\bar{1}0)$ pole figures of Layers 1 and 2 were indicative of the preferred crystal orientation. In all $(10\bar{1}0)$ pole figures of Layers 1 and 2, three poles, 60° apart and lying on the equator, could be seen clearly or inferred (Fig. 7). This supports the contention that the hexagonal crystalline phase was present and that the *c*-axis was aligned parallel with the injection direction. The DSC data (Table I) showed no evidence of a high-melting-point, chain-extended phase, as has been observed

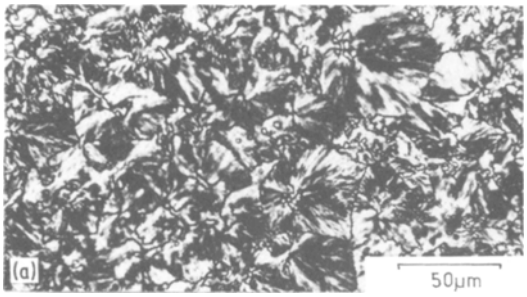

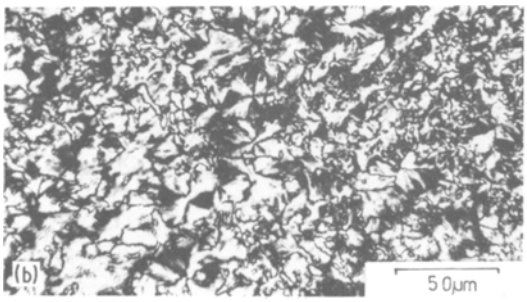

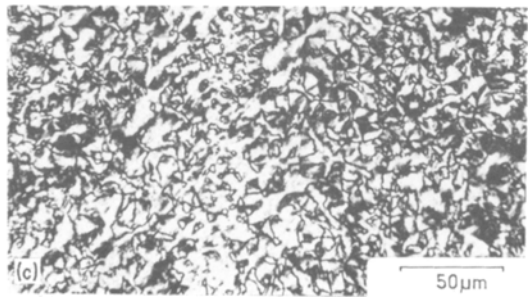

Figure 9 The influence of processing conditions on the morphology of Layer 5. Barrel temperatures: (a) 493 K, (b) 473 K, (c) 453 K.

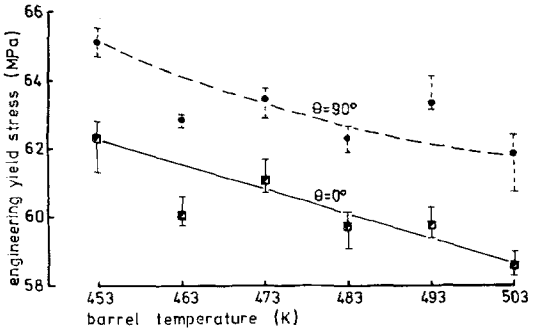

Figure 10 The influence of barrel temperature on the engineering yield stress for tensile samples cut parallel and perpendicular to the direction of injection.

in injection mouldings of high density polyethylene [29, 46]; for blown films of polyoxymethylene homopolymer, DTA melting data showed no higher-melting component, in fact the melting point of the film increased on subsequent re-meltings [47], a result also obtained in this study. To accord with the above data it is proposed that Layer 1 formed from melt which was oriented by extensional flow at the melt front [36], that nucleation in this outside layer was spontaneous and dominating because of the highly oriented melt [48, 49] and the high cooling rate, and that the structure is a stacked lamellae one with the chain axis parallel to the direction of injection. This structure is similar to that observed by Clark [11] in the surface of specimens of injection-moulded acetal homopolymer. In addition, the fast rate of cooling of Layer 1 may be responsible for the "single crystal" texture observed at low barrel temperatures (see Figs 4 and 7) in Layers 1 and 2.

5.2.2. Layer 2

Viewed between crossed polars, the microstructure was spherulitic but growth was constrained to a direction away from the cold mould wall (Figs 3 and 7). This microstructure is similar, both in form and position, to that observed by Menges *et al.* [46] in injection mouldings of high-density polyethylene. As noted above, the (1 0 $\bar{1}$ 0) pole figures of Layers 1 and 2 indicated that the chain axis was aligned parallel with the injection direction. It is postulated that the melt that formed this second layer was oriented by flow at the melt front, and that this preferred chain-axis orientation was preserved on cooling to give the layer its bi-refringence and Layers 1 and 2 the texture they possess (Fig. 4). The presence of Layer 1 reduced the cooling rate in Layer 2, delayed crystallization and allowed some melt relaxation. The reduced cooling rate and the loss of some melt orientation together allowed growth of oriented spherulites from the nuclei that had formed. In quiescent melts the presence of a large temperature gradient can induce the so-called "transcrystalline" texture [50–54], where growth is parallel to the largest temperature gradient and the fast growth axis of the crystal aligns parallel to the largest temperature gradient [50]. In Layer 2 the growth of the spherulites away from the cold mould wall mirrors the "transcrystalline" morphology, with the oriented spherulite nucleation density controlled by the barrel temperature. For the "transcrystalline" texture and morphology, growth is preferred to nucleation.

5.2.3. Layer 3

The extent of the finely structured Layer 3 as a function of distance from the gate was examined at all barrel temperatures; in every case Layer 3 was present near, but absent far, from the gate (Fig. 13). This is the only easily interpretable clue as to the origin of Layer 3, as the (1 0 $\bar{1}$ 0) pole figure of Layer 3 (Fig. 4), the polarized light photomicrographs (Fig. 3) and the DSC melting data (Table I) are difficult to interpret. Computer studies of mould filling have indicated an increasing stationary skin thickness with time during mould filling [38, 39]. Structure 3 may therefore represent the growth of the stationary skin during mould filling; this implies that the melt that formed Layer 3 did not undergo flow at the melt front, but deposited on to the already frozen skin from the core flowing melt. This continual "laying down" may have precluded the growth of spherulites and account for the fine morphology observed (Figs 3 and 13).

The (1 0 $\bar{1}$ 0) pole figures of Layer 3 are difficult to interpret, but one avenue of approach is to postulate that the orthorhombic phase was present, the orthorhombic (1 1 0) and (0 2 0) reflections, which have Bragg angles close to the hexagonal (1 0 $\bar{1}$ 0) [21], contributing to the final texture. The high shear stresses present at the stationary skin/core flowing melt interface [36, 37, 46] could have induced a transformation [22, 26]. However, the observed angular separation of 135° between the two observed poles (see Table I), and the absence of exo- or endothermic peaks at the expected temperature of transformation (333 K

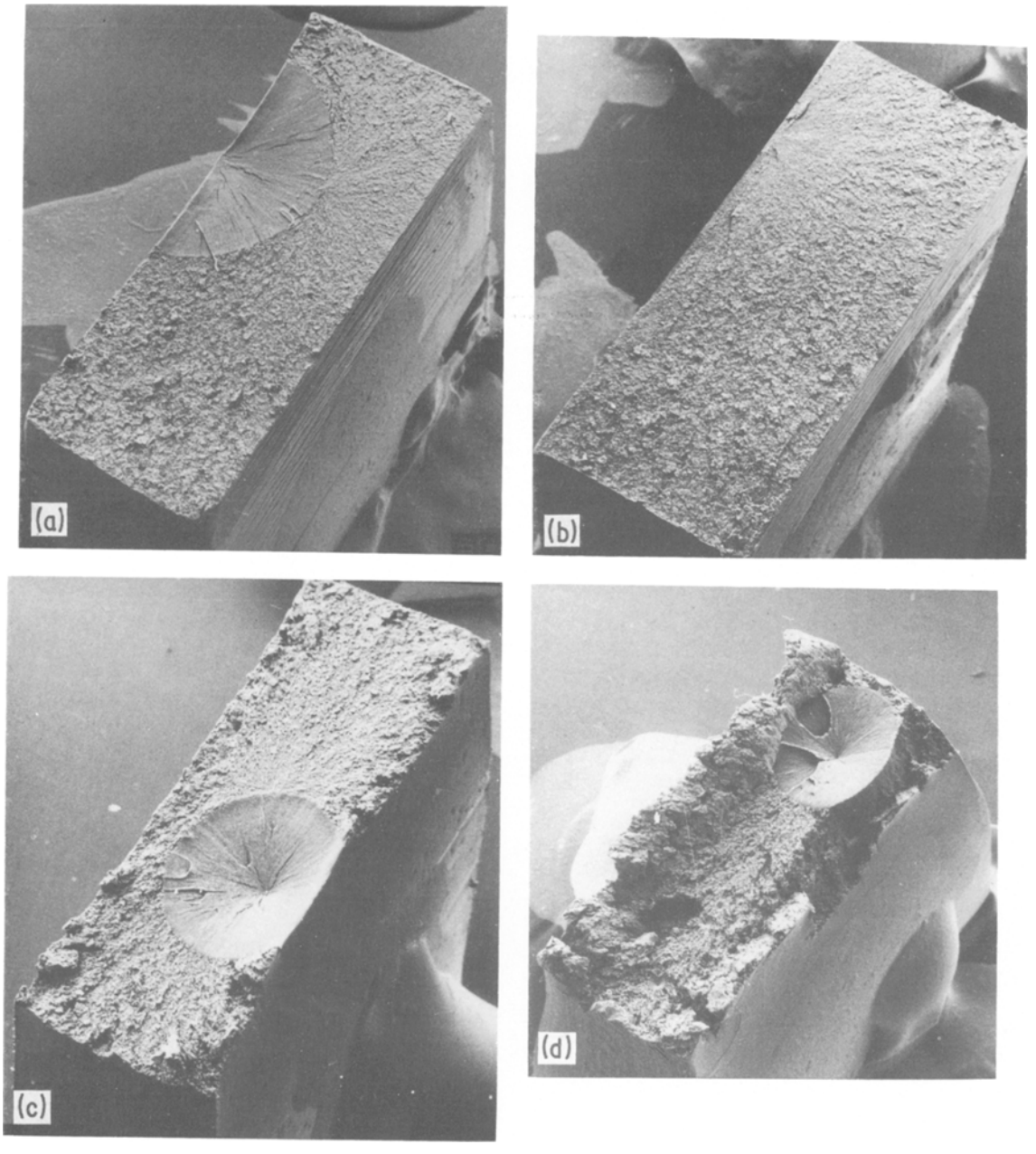

Figure 11 Scanning electron micrographs of fracture surfaces of tensile specimens. (a) and (b) Samples cut perpendicular ($\alpha = 90°$) to the injection direction, showing fracture initiating at or near the surface in the highly oriented layers and exhibiting crazing. (c) and (d) Samples cut parallel ($\alpha = 0°$) to the injection direction, showing failure initiating in the centre equiaxed layers. The higher barrel temperature moulding exhibits more local necking.

[21]), do not indicate positively the presence of the orthorhombic phase.

5.2.4. Layer 4

The morphology of Layer 4 exhibited a small amount of preferred orientation (see Fig. 3), but the $(1\,0\,\bar{1}\,0)$ pole figures and the value of $\langle\cos^2\theta_{md}\rangle$ showed little preferred c-axis orientation. The morphology of this layer indicates that nucleation took place under small shear stresses [46, 48]. The melt that formed Layer 4 flowed between the frozen skins, the shear stresses present in the core flowing melt [36, 37, 46] introducing the bi-refringence morphology. The perfection of

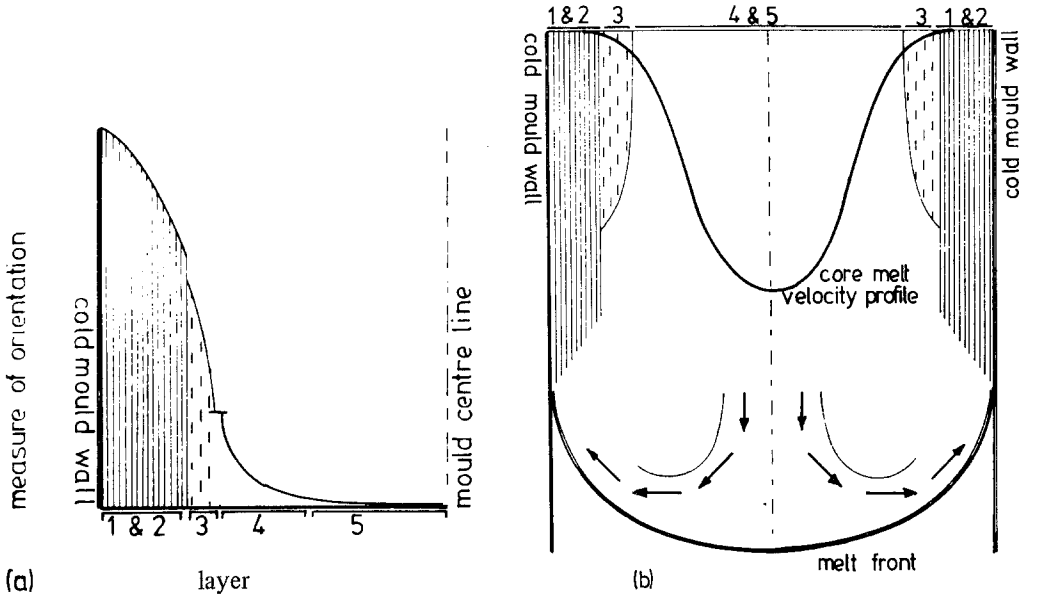

Figure 12 (a) Schematic presentation of the orientation within a moulded plaque. The extent of the preferred molecular orientation is as obtained from X-ray pole figure and moulded plaque morphology analysis. (b) Melt flow at the melt front, to give the highly oriented outer layers, and the melt flow behind the front and between the frozen skins to give the lightly oriented inner layers.

the spherulites in Layer 4 indicates crystallization under moderate rates of quenching [55].

5.2.5. Layer 5

Layer 5 showed no anistropy of texture or morphology, the morphology being coarse spherulitic. The melt to form Layer 5 underwent little or no shear [36, 37, 46] in flowing down the centre of the cavity. The cooling rate was low to give coarse structure spherulites [55].

Table I tabulates the five layers found within the acetal copolymer plaque mouldings, and describes their texture and microstructure. Table II identifies, for the five layers, the processes whereby the preferred orientation was induced, and notes the influence of thermal history on morphology.

5.3. Influence of barrel temperature on layer extent

Increasing the barrel temperature reduced the extent of oriented Layers 1, 2 and 3, but increased the extent of Layers 4 and 5. In Section 5.2 it was proposed that the melt for Layers 1 and 2 underwent extensional flow at the melt front, while Layer 3 was deposited continuously during mould filling. Layers 4 and 5 formed from the core flowing melt. Increasing moulding barrel temperature reduced melt viscosity, and the reductions in the melt viscosity reduced the extent of Layers 1 and 2 by reducing the volume of melt undergoing extensional flow at the melt front. In addition, the extra heat content of the melt at the higher barrel temperatures decreased the extent of Layer 1 by reducing the cooling rate and allowing growth

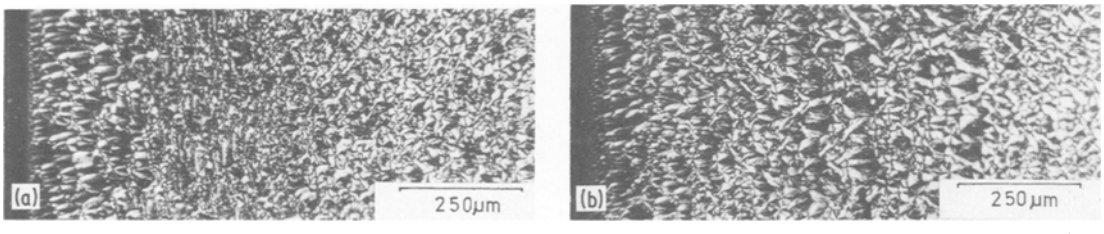

Figure 13 Optical photomicrographs of the 483 K barrel temperature moulding, taken from (a) near and (b) far from the gate, showing how the presence of Layer 3 changes.

TABLE II Microstructure–melt history interrelations for the identified layers

Layer	1	2	3	4	5
Preferred orientation	Highly bi-refringent, chain axis aligned with injection direction		Chain axis aligned with injection direction	Some preferred morphological	Little preferred orientation
Origin of preferred orientation	Chain axis orientation from extensional flow of melt at melt front		Shear in melt at stationary skin–core melt interface	Shear in core flowing melt	
Microstructure	Stacked lamellae	Anistropically shaped spherulites with preferred growth direction away from mould wall	Sheared	Spherulitic with some oriented material	Course, large spherulites
Cooling rate and effect	Very fast; preserves flow-induced preferred chain orientation	Fast, retaining preferred chain orientation and inducing preferred growth	Cooling of core flowing melt reduced melt viscosity to precipitate layer	Medium, some nucleation from shear in core flowing melt	Low, favouring large, course spherulites
Nucleation or growth	Nucleation preferred	Growth preferred, parallel with large temperature gradient	–	Even, microstructure anistropy induced by shear of melt	Small nucleation density, growth preferred

from the nuclei (homo- or heterogeneous), thus producing Layer 2 in perference to 1.

The extent of Layer 3 decreased with increasing barrel temperature (Fig. 6a). In Section 5.2 it was postulated that Layer 3 formed from cooled core-flowing melt (when the viscosity of the melt prohibited flow). Increasing barrel temperature increased melt heat content and reduced melt viscosity, therefore decreasing the rate of deposition and the extent of Layer 3. Previous studies on the microstructure of injection-moulded semicrystalline thermoplastics with complex, multilayered structures have all shown highly oriented outer layers decreasing in extent with increasing barrel temperature [6, 8, 10, 14]. Computer studies of mould filling have also indicated that the extent of the slow-moving or stationary skin decreases with increasing barrel temperature [38].

Layers 4 and 5 increased with increasing barrel temperature (Fig. 6b), Layer 4 appearing to attain a constant value. The increase in the extent of Layer 5 results from a reduced skin thickness and the extra melt-heat content, the latter allowing melt relaxation and favouring the equiaxed microstructure. The increases in the extent of the lightly oriented Layer 4 with increasing barrel temperature are difficult to explain. At low barrel temperatures skin thickness was at its greatest, the narrow channel for the core flowing melt increasing the shear, and also increasing the melt temperature to allow melt relaxation and favour Structure 5. At the higher melt temperatures the skin thickness was reduced to reduce the shear and keep the melt temperature lower. Computer studies have indicated self-heating [39].

5.4. The influence of barrel temperature on the microstructure of Layers 1 to 5

In general, increasing barrel temperature increased spherulite size in Layers 2, 4 and 5, and reduced the preferred orientation within Layers 1 and 2 (see Fig. 7) and Layer 4 (see Fig. 8). Increasing barrel temperature increased melt-heat content and reduced the cooling rate at those temperatures where the nucleation density is low and growth is fast [56], thus favouring growth to nucleation to increase spherulite size. The lowering of the cooling rate also favoured a coarser spherulitic structure in Layer 5, a result consistent with previous studies [55]. In Layers 1 and 2, the loss of preferred crystal orientation with increasing barrel temperature, which has been observed in a previous study [14], was due primarily to melt relaxation, the extra heat content and temperature of the melt delaying cooling and reducing relaxation times.

5.5. Mechanical properties of mouldings

An equiaxed, semicrystalline polymer (that is, one without preferred crystalline orientation) will exhibit mechanical isotropy on the macroscopic level. The introduction of a chain-extended phase and preferred orientation to the macromolecules and lamellae will introduce mechanical anistropy. In this study of injection-moulded plaques of an acetal copolymer, the absence of a phase of high melting point [29] infers that no chain-extended component was present. The $(1\,0\,\bar{1}\,0)$ pole figures in Fig. 4 show preferred texture in the outer layers with the chain axis oriented predominantly (in the crystalline phase) parallel with the injection direction. For injection mouldings of an acetal homopolymer, Clark [11] proposed, from the evidence of transmission electron micrographs of replicas taken from the surface of mouldings, that the layer next to the mould wall was composed of stacked lamellae. The single-crystal-like texture of the low barrel temperature mouldings (Fig. 7) and the absence of any resolvable morphology in the outer layers (Fig. 3) leads to the same conclusion, that in these injection mouldings the outer, most highly oriented layer was composed of a stacked lamellae structure. No small-angle X-ray photomicrographs were taken to determine the exact form of stacking (for instance parallel or roof-top [57]). However, it is assumed that the observed mechanical anistropy of these injection mouldings is due to the presence of the outer oriented layers, and that the arrangement of the lamellae within these layers determines the mechanical response.

Takayanagi and co-authors [58] have examined the mechanical response of lightly oriented (draw ratio less than 8) semicrystalline polymers. The mechanical response of these polymers was explained in terms of a model which simplified the arrangement of the crystalline and amorphous phases into a series- and parallel-type arrangement. This model can be applied to these injection-moulded acetal copolymer mouldings to explain their mechanical anistropy. The higher values for both yield stress and short-term modulus perpendicular to the injection direction, which has been observed in previous studies [8, 16, 59], may be ascribed to the presence of oriented lamellae. The lamellae are, at this testing temperature, the stiff phase, the amorphous material being considerably more compliant [56, 57, 60]. To pull perpendicular rather than parallel to the injection direction is to pull on the larger dimension of the stiff crystalline phase, to simulate a parallel-type loading [57, 58] and thus to give the higher modulus and yield stress. The decrease in both the parallel and perpendicular yield stress with increasing barrel temperature (Fig. 10) may be associated with the volume of oriented material (Fig. 14). In the perpendicular case the decrease in the yield stress with increasing barrel temperature was associated with the volume of oriented lamellae. In the parallel case the higher barrel temperature mouldings gave the lower yield stress; this behaviour may be associated with the number of oriented macromolecules in the amorphous phase. At low barrel temperatures it may be expected that more macromolecules in the amorphous phase were aligned parallel with the injection direction, due to a faster rate of cooling preserving macromolecular orientation. Therefore, both the orientation of the macromolecules (in the amorphous phase) and the lamellae influence mechanical properties, and any decrease in the volume of oriented material will decrease both yield stresses, parallel and perpendicular, for these moderately oriented materials.

The fracture surfaces of tensile specimens taken from the injection-moulded plaques clearly reflect the underlying microstructure of the mouldings. Tensile specimens, cut and tested perpendicular to the injection direction, first exhibited surface crazing, then failed in a brittle manner with fracture initiating in the outer highly oriented layers (Fig. 11a and b). The presence of the surface crazing and the site of fracture infer that in the perpendicular case the ability of the outer oriented material to absorb strain was reduced. This lack of ability to absorb strain may reflect a restriction on

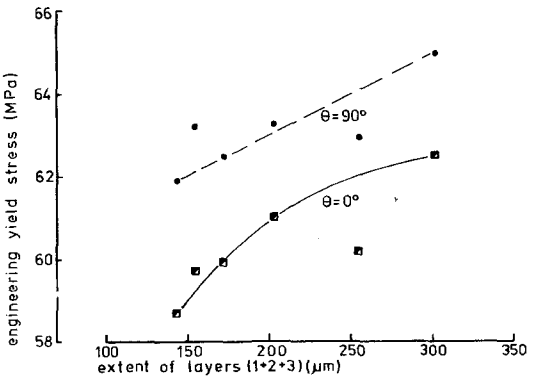

Figure 14 The influence of the extent of the oriented layers (Layers 1, 2 and 3) on the engineering yield stress, for the tensile axis aligned parallel ($\alpha = 0°$) and perpendicular ($\alpha = 90°$) to the direction of injection.

the lamellae to rotate to absorb strain. Since the outer layers carried a higher fraction of the load, failure of these layers precipated total fracture of the perpendicular tensile specimen. Tensile specimens cut and tested parallel to the injection direction failed in a different manner. There was no surface crazing and fracture initiated in the centre of the moulding (Fig. 11c and d). Tested parallel with the injection direction, the fracture of the tensile specimens was initiated in the lightly oriented inner layers. This movement of fracture initiation site supports the observation that the ability of the outer oriented layers to draw depends upon loading direction relative to the preferred orientation.

6. Conclusions

A substantial amount of work was undertaken to study, in a systematic manner, the relationships between processing conditions, overall structure, the microstructure of individual layers and the mechanical properties of injection-moulded plaques of an acetal copolymer. Correlations exist between processing conditions, overall structure and mechanical properties, so that the performance of a moulding can be controlled via the processing conditions used during fabrication. The detailed study and analysis of the texture and microstructure of the individual layers within the mouldings was shown to relate to a possible mode of melt flow during mould filling (the model of mould filling was that of Tadmor [36]), the rate of cooling of the melt at various points through the thickness of the moulding also influencing final microstructure and texture of the layers.

Specifically, it can be concluded from this study that:

(a) At all barrel temperatures the microstructure of the mouldings was layered and symetrical about the centre line. Five layers were identified, the outer three possessed significant preferred chain-axis orientation, while the inner layers, Layers 4 and 5 exhibited little preferred orientation.

(b) The melt that formed the outermost layers Layers 1 and 2, probably underwent extensional flow at the melt front, thus inducing a significant preferred chain-axis orientation which was retained by the quenching effect of the cold mould wall. The pole figures for Layers 1 and 2 infer a single-crystal, as opposed to fibre-like, texture [6, 29]. The transcrystalline morphology may result from the rapid quenching giving preferred growth direction. Layer 3 possessed a sheared microstructure and was probably deposited as the viscosity in the core flowing melt increased as that melt cooled. Layers 4 and 5 formed from core flowing melt, and possessed little preferred orientation.

(c) Increases in barrel temperature relaxed the texture and preferred chain-axis orientation in Layers 1 and 2 as the melt had longer to relax, with shorter relaxation times, before crystallization. The size of the spherulites in Layers 5, 4 and 2 (anistropically shaped in this layer) increased with barrel temperature increases, reflecting the preference for spherulite growth to nucleation at the slower cooling rates.

(d) Increases in barrel temperature reduced the extent of the highly oriented layers (Layers 1, 2 and 3) and increased the extent of Layers 4 and 5.

(e) At all barrel temperatures, the engineering yield stress perpendicular to the injection direction was greater than that parallel to the injection. This behaviour was interpreted in terms of a composite model.

(f) Increases in the barrel temperature did not influence modulus but reduced the engineering yield stress both parallel and perpendicular to the injection direction. The engineering yield stress correlated with the extent of the highly oriented layers, Layers 1, 2 and 3.

(g) The site of initiation of failure was at the edge for the tensile samples pulled perpendicular to the injection direction, and at the centre for those pulled parallel, the preferred chain-axis orientation controlling initiation site.

Acknowledgements

The work for this paper was carried out principally in the Department of Metallurgy and Materials Science at The University of Liverpool. The author wishes to thank the University for financial support and Professor D. Hull for provision of laboratory facilities and valuable discussions. The author is indebted to the Rubber and Plastics Research Association, Shawbury, for supply of material and the use of moulding equipment and to Dr J. Preedy of BP Ltd for carrying out work on the X-ray characterization. Finally the author would like to thank Professor M. Bevis for support and valuable discussions.

References

1. Z. MENCIK and A. J. CHOMPFF, *J. Polymer Sci. Phys.* **12** (1974) 977.

2. J. E. CALLEAR and J. B. SHORTHALL, *J. Mater. Sci.* **12** (1977) 141.
3. S. Y. HOBBS and C. F. PRATT, *J. Appl. Polymer Sci.* **19** (1975) 1701.
4. D. P. RUSSEL, PhD. Thesis, Cambridge University, 1977.
5. M. FLEISSNER and E. PASCHKE, *Kunststoffe* **61** (1971) 195.
6. W. HECKMANN and G. SPILGIES, *Kolloid Z.u.Z. Polymere* **250** (1972) 1150.
7. G. WÜBKEN, PhD. Dissertation, Technical High School, Aachen, May 1974.
8. M. R. KANTZ, H. D. NEWMAN and F. H. STIGLE, *J. Appl. Polymer Sci.* **16** (1972) 1249.
9. S. J. HENKE, C. E. SMITH and R. F. ABBOT, *Polymer Eng. Sci.* **15** (1975) 79.
10. D. R. FITCHMUN and Z. MENCIK, *J. Polymer Sci. Phys.* **11** (1973) 951 and 973.
11. E. S. CLARK, *SPE J.* **23(7)** (1967) 46.
12. *Idem, Appl. Polymer Symp.* **20** (1973) 325.
13. T. W. OWEN and D. HULL *Plastics and Polymers* **41** (February 1974) 19.
14. J. BOWMAN, N. HARRIS and M. BEVIS, *J. Mater. Sci.* **10** (1975) 63.
15. J. BOWMAN and M. BEVIS, *Plastics and Rubber: Materials and Applications* **1** (1976) 177.
16. J. BOWMAN and M. BEVIS, unpublished work.
17. E. O. ALLEN and G. W. VAN PUTTE, *Plastics Eng.* **30** (July 1974) 37.
18. D. E. SCHERPEREEL, *Plastics Eng.* (December 1976) 46.
19. E. CLARK, *Plastics Eng.* (March 1974) 74.
20. E. BOHME, *Kunststoffe* **60** (1970) 273.
21. E. P. CHANG, R. W. GRAY and N. G. McCRUM, *J. Mater. Sci.* 8 (1973) 397.
22. J. E. PREEDY and E. J. WHEELER, *Nature* **236** (1972) 60.
23. E. H. ANDREWS and G. E. MARTIN, *J. Mater. Sci.* 8 (1973) 1315.
24. M. DROSCHER, G. LIESER, H. REIMANN and G. WEGNER, *Polymer* **16** (1975) 497.
25. G. A. CARAZZOLO and M. J. MAMMI, *J. Polymer Sci. (A)* **1** (1963) 965.
26. N. HARRIS and M. BEVIS, *J. Mater Sci.* **10** (1975) 539.
27. K. O'LEARY and P. H. GEIL, *J. Macromolec. Sci. Phys.* **132** (1968) 261.
28. M. J. MILES and N. J. MILLS, *J. Mater. Sci.* **10** (1975) 2092.
29. W. HECKMANN and U. JOHNSON, *Colloid Polymer Sci.* **252** (1974) 826.
30. B. D. CULLITY, "Elements of X-ray Diffraction", (Addison-Wesley, New York, 1956).
31. L. G. SCHULTZ, *J. Appl. Phys.* **20** (1949) 1030.
32. D. LEWIS, E. J. WHEELER, W. F. MADDONS and J. E. PREEDY, *J. Appl. Crystallog.* **4** (1971) 55.
33. G. L. WILKES, *Adv. Polymer Sci.* 8 (1971) 91.
34. C. R. DESPER and R. S. STEIN, *J. Appl. Phys.* **37** (1966) 3990.
35. R. L. BALLMAN and H. L. TOOR, *Modern Plastics* **38** (October 1960) 113.
36. Z. TADMOR, *J. Appl. Polymer Sci.* **18** (1974) 1753.
37. J. L. BERGER and C. G. GOGOS, *Polymer Eng. Sci.* **13** (1973) 102.
38. P-C. WU, C. F. HUANG and G. G. GOGOS, *ibid* **14** (1974) 223.
39. H. A. LORD and G. WILLIAMS, *ibid* **15** (1975) 553.
40. P. THIENEL and G. MENGES, *ibid* **18** (1978) 314.
41. J. L. WHITE and H. B. DEE, *ibid* **14** (1974) 212.
42. J. L. WHITE, Ibid **15** (1975) 44.
43. L. R. SCHMIDT, *ibid* **14** (1974) 797.
44. R. S. SPENCER and G. D. GILMORE, *J. Colloid Sci.* **6** (1951) 118.
45. J. L. S. WALES, J. VAN LEEUWEN and J. VAN DER VIJGH, *Polymer Eng. Sci.* **12** (1972) 358.
46. G. MENGES, G. WUBKEN and B. HORN, *Colloid Polymer Sci.* **254** (1976) 267.
47. C. A. GARBER and E. S. CLARK, *J. Macromolec. Sci. Phys.* **B4** (1970) 499.
48. E. H. ANDREWS, *Proc. Roy. Soc.* **A277** (1964) 562.
49. T. W. HAAS and B. MAXWELL, *Polymer Eng. Sci.* 9 (1969) 225.
50. R. K. EBY, *J. Appl. Phys.* **35** (1964) 2720.
51. D. R. FITCHMUN and S. NEWMAN, *J. Polymer Sci.* **A2** 8 (1970) 1545.
52. A. M. CHATTERJEE, F. P. PRICE and S. NEWMAN, *J. Polymer Sci. Phys.* **13** (1975) 2369.
53. *Idem, ibid* (1975) 2385.
54. *Idem, ibid* (1975) 2391.
55. C. F. HAMMER, T. A. KOCH and J. F. WHITNEY, *J. Appl. Polymer Sci.* **1** (1959) 169.
56. D. W. KREVELEN, "Properties of Polymers", (Elsevier, Amsterdam, 1972).
57. M. KAPUSCINSKI, I. M. WARD and J. SCANLAN, *J. Macromolec. Sci. Phys.* **B11** (1975) 475.
58. M. TAKAYANAGI, K. IMADA and T. KAJIYAMA, *J. Polymer Sci.* **Part C15** (1966) 263.
59. E. PASCHKE, *Kunststoffe* **60** (1970) 187.
60. E. H. ANDREWS, *Pure Appl. Chem.* **39** (1974) 179.

Received 28 July and accepted 2 September 1980.